The Poly(Adenosine Diphosphate-Ribose) Polymerase Inhibitor PJ34 Reduces Pulmonary Ischemia-Reperfusion Injury in Rats

Go Hatachi,[1] Tomoshi Tsuchiya,[1] Takuro Miyazaki,[1] Keitaro Matsumoto,[1] Naoya Yamasaki,[1] Naoyuki Okita,[2] Atsushi Nanashima,[1] Yoshikazu Higami,[2] and Takeshi Nagayasu[1,3]

Background. Ischemia-reperfusion (I/R) injury after lung transplantation causes alveolar damage, lung edema, and acute rejection. Poly(adenosine diphosphate-ribose) polymerase (PARP) is a single-stranded DNA repair enzyme that induces apoptosis and necrosis after DNA damage caused by reactive oxygen species. We evaluated tissue protective effects of the PARP inhibitor (PARP-i) PJ34 against pulmonary I/R injury.
Methods. Rats (total n=45) underwent a thoracotomy with left hilar isolation and saline administration (sham group) or thoracotomy with hilar clamping and saline administration (I/R group) or PJ34 administration (PARP-i group). Parameters were measured for 7 days after reperfusion.
Results. Pathologic analysis revealed that reperfusion injury was drastically suppressed in the PARP-i group 2 days after reperfusion. Terminal deoxynucleotide transferase-mediated deoxyuridine triphosphate nick-end labeling–positive cells were significantly decreased in the PARP-i group compared to the I/R group ($P<0.05$). Accordingly, the wet-to-dry lung ratio in the I/R group was significantly higher compared with the PARP-i group ($P=0.025$). Four hours after reperfusion, serum tissue necrosis factor-α and interleukin-6 were significantly suppressed in the PARP-i group compared with the I/R group ($P<0.05$). Serum derivatives of reactive oxygen metabolites increased quickly and remained high in the I/R and PARP-i groups from 4 hr until 7 days after reperfusion. Interestingly, the serum biologic antioxidant potential in the PARP-i group was significantly higher than that in the I/R group from day 2 until day 7.
Conclusion. The PARP-i decreased inflammation and tissue damage caused by pulmonary I/R injury. These beneficial effects of the PARP-i may be correlated with its antioxidative efficacy.

Keywords: Ischemia-reperfusion injury, PARP inhibitor, PJ34, Antioxidants.

Ischemia-reperfusion (I/R) injury remains one of the major problems in lung transplantation; it causes disorders of the alveoli and the vascular endothelium and sequentially induces pulmonary edema and acute rejection (*1, 2*). Therefore, suppression of I/R injury is expected to prevent or reduce lung disorders after lung transplantation.

Ischemia-reperfusion overactivates poly(adenosine diphosphate-ribose) polymerase (PARP). Poly(adenosine diphosphate-ribose) polymerase1 and PARP2 are involved in replication, DNA repair, and cell death (*3–5*) (**Figure S1, SDC**, http://links.lww.com/TP/B25). In response to I/R, the nuclear factor (NF)-κB-PARP1complex induces the

transcription of proinflammatory genes in macrophages. The subsequent production of nitric oxide and reactive oxygen species triggers DNA strand breaks. Poly(adenosine diphosphate-ribose) polymerase is dramatically activated by DNA breaks and then catalyzes poly(adenosine diphosphate ribosyl)ation on substrate proteins in regions of DNA damage, events that require efficient recruitment of DNA repair factors to the loci (6, 7). The overactivation of PARP decreases cellular nicotinamide adenine dinucleotide and adenosine triphosphate (ATP) levels, resulting in necrotic cell death (8–11). Activated PARP also modulates inflammatory signaling cascades and apoptotic pathways by reduction of the mitochondrial membrane potential and the release of apoptosis-inducing factor (12–16). Therefore, inhibition of PARP is believed to reduce cell death in inflamed organs (17).

PJ34 (*N*-(6-oxo-5,6-dihydro-phenanthridin-2-yl)-*N*, dimethylacetamide) is a potent PARP inhibitor (PARP-i) with strong tissue protective effects in rat models of cerebral stroke, heart transplantation, and liver I/R injury as well as in a mouse hindlimb ischemia model (18, 19). The mechanism of the tissue protective effect is suppression of PARP activation and decreased competitive binding of PARP with nicotinamide adenine dinucleotide, resulting in increased ATP and preservation of the total adenylate pool. As a result, necrotic and apoptotic cell populations are decreased.

In the present study, we evaluated the effect of the PARP-i PJ34 in pulmonary I/R injury in a rat pulmonary hilar clamping model. Because PARP-is are antioxidants, the oxidative stress levels and antioxidant potential levels were measured for 7 days after reperfusion.

RESULTS

Active PARP Protein Levels in the Lung

Full-length PARP (113 kDa) is cleaved into the active 89-kDa form in the early apoptotic phase. Western blotting revealed that the cleaved PARP protein was increased 2 days after reperfusion in the I/R group; however, the level in the PARP-i administrated group remained as low as in the sham group (Fig. 1A).

Concentration of ATP in the Tissues

In the I/R group, the concentration of ATP at 2 days after reperfusion was significantly lower than that in the other two groups ($P<0.03$). No significant differences were noted among the three groups at other time points after reperfusion (Fig. 1B).

Wet-to-Dry Lung Ratio

Two days after reperfusion, the wet-to-dry (W/D) lung ratio in I/R group is significantly higher than those in the sham and PARP-i groups ($P<0.03$) (Fig. 1C), indicating that severe lung edema was induced in the I/R group but suppressed in the PARP-i group by PJ34.

Histologic Findings and Blood Chemistry of Liver Enzymes

Hematoxylin-eosin (H&E) staining showed that the 1-hr ischemia induced severe inflammation in the I/R group 2 days after reperfusion. However, in the PARP-i group, the degree of inflammation was reduced to the same level as in the sham group (Fig. 2A). No obvious systemic inflammation was observed in the liver or kidney of any group 2 days after reperfusion (Fig. 2B and C).

To measure the potential damages to liver, aspartate transferase (AST), alanine transferase (ALT), and lactate dehydrogenase were measured. Two days after reperfusion, AST levels were significantly higher in the I/R and the PARP-i group compared to the sham group. No significant differences were observed between the I/R and PARP-i group at any time point (Fig. 2D). No differences in ALT or lactate dehydrogenase were seen at any time points among any groups (Fig. 2E and F).
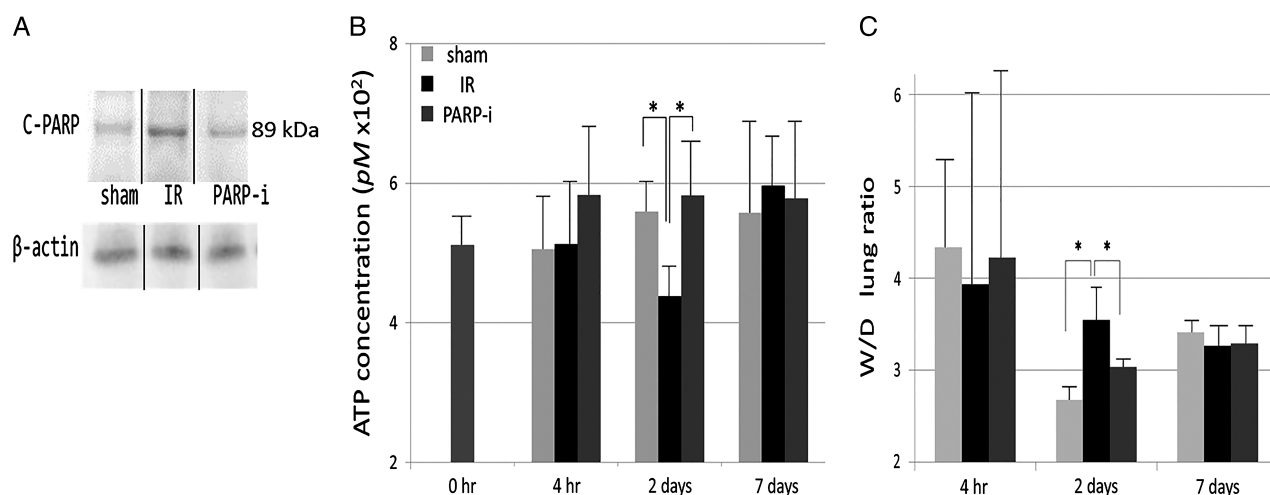
FIGURE 1. A, Western blot of the cleaved active form of PARP at 2 days after reperfusion. B, ATP concentration in the three groups before treatment, 4 hr, 2 days, and 7 days after reperfusion. At 2 days after reperfusion, there were significant differences between I/R group and other 2 groups (*$P<0.05$). C, W/D lung ratio at 4 hr, 2 days, and 7 days after reperfusion. At 2 days after reperfusion, there were significant differences between I/R group and other 2 groups (*$P<0.05$). Data were represented as mean±SD. (n=5). ATP, adenosine triphosphate; W/D, wet-to-dry; PARP, poly(adenosine diphosphate-ribose) polymerase; SD, standard deviation.
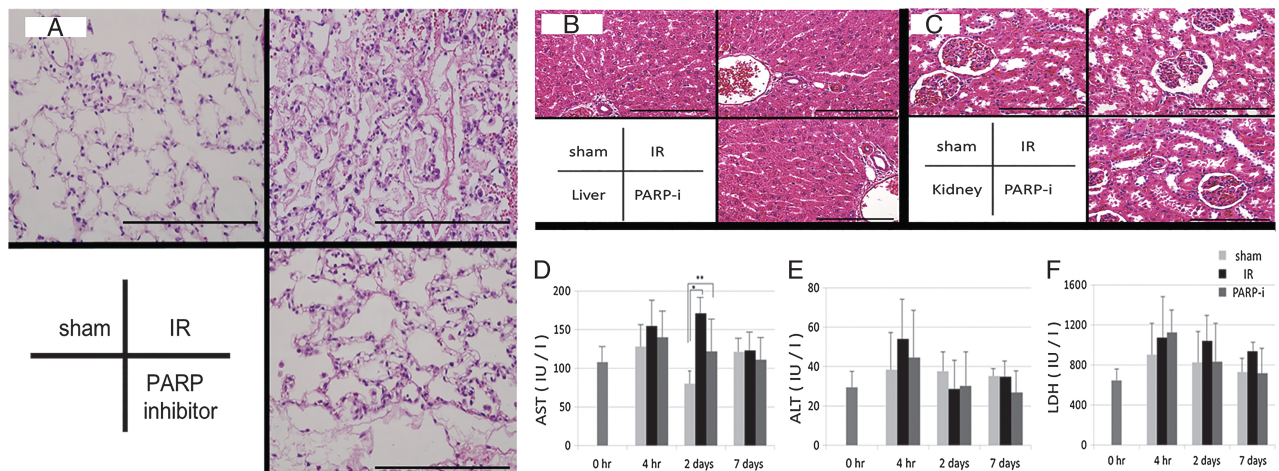
FIGURE 2. A, representative pulmonary histologic findings of hematoxylin-eosin staining 2 days after reperfusion. Two days after reperfusion, I/R injury caused severe inflammation. Scale bar, 200 μm. Representative hepatic (B) and renal (C) histologic findings of hematoxylin-eosin staining at day 2. Changes in AST (D), ALT (E), and LDH (F) 4 hr, 2 days, and 7 days after reperfusion. There was a significant difference between sham group and other 2 groups (*$P<0.03$; **$P<0.05$). However, no significant difference was observed between I/R group and PARP-i group. I/R, ischemia-reperfusion; AST, aspartate transferase; ALT, alanine transferase; LDH, lactate dehydrogenase; PARP-I, PARP, poly(adenosine diphosphate-ribose) polymerase inhibitor.

Terminal Deoxynucleotide Transferase-Mediated Deoxyuridine Triphosphate Nick-End Labeling Staining

Morphologically, most of the terminal deoxynucleotide transferase-mediated deoxyuridine triphosphate nick-end labeling (TUNEL)-positive cells were inflammatory cells. However, TUNEL-positive cells were also observed in alveolar septa (Fig. 3A-e). Fluorescent immunostaining also revealed that TUNEL-positive cells were observed in alveolar septa and capillaries in the I/R group (Fig. 3A-f).

The TUNEL-positive cells were more frequently observed in I/R group (Fig. 3A-a, A-d, and A-g). The number of TUNEL-positive cells was significantly higher in the I/R group than that in the other two groups ($P<0.05$) (Fig. 3B).

The Inflammatory Cytokines: Tissue Necrosis Factor-α and Interleukin-6

Serum tissue necrosis factor (TNF)-α levels were increased significantly in the I/R group compared to the other two groups at 4 hr after reperfusion ($P<0.05$) (Fig. 4A). At 4 hr and 2 days after reperfusion, serum interleukin (IL)-6 was increased in the I/R group compared to the other two groups (Fig. 4B). A significant difference in IL-6 levels between the I/R group and the other two groups was observed 2 days after reperfusion (Fig. 4; $P<0.05$). Neither TNF-α nor IL-6 was detectable at 7 days after reperfusion in any of the three groups (Fig. 4A and B). Similar results were observed for messenger RNA (mRNA) expression of IL-6 and TNF-α (Fig. 4C and D).

Oxidative Status–Related Markers

Derivatives of reactive oxygen metabolites (d-ROMs) were drastically increased until 2 days after reperfusion and then decreased. The I/R and PARP-i groups had significantly higher d-ROM levels compared to the sham group from 3 days to 7 days (Fig. 5A). Biologic antioxidant potential (BAP) was significantly increased in the I/R group 4 hr after reperfusion ($P<0.03$) and then decreased to the pre-ischemia level. Interestingly, the peak of the BAP level in the PARP-i group was delayed until 2 days and remained high throughout the week (Fig. 5B). Significant differences in BAP levels between the PARP-i group and I/R group were observed until 5 days. The oxidative stress index 2 days after reperfusion was 0.90 ± 0.04 in the sham group, 1.50 ± 0.07 in the I/R group, and 0.92 ± 0.05 in the PARP-i group. The PARP-i group had a significantly lower oxidative stress index than the I/R group ($P<0.03$) (Fig. 5C), and this difference remained until 7 days after reperfusion.

DISCUSSION

The present results clearly illustrate the tissue protective effect of PJ34 in pulmonary I/R injury. Histologic analysis revealed that PJ34 suppressed lung edema and inflammatory cell infiltration. The TUNEL-positive cells were observed in the I/R group but were rarely observed in the PARP-i group, indicating that tissue damage was lower in the PARP-i group.

The results were consistent with I/R models of the brain, heart, and liver. The beneficial effects of a PARP-i on neutrophil infiltration (20) and brain hemorrhage (21) have been demonstrated in brain ischemia models. Poly(adenosine diphosphate-ribose) polymerase activation contributes to the expression of P-selectin and intracellular adhesion molecule (ICAM)-1 (22). Because a PARP-i reduces the immunostaining of P-selectin and ICAM-1 1 hr after reperfusion (23), PARP-i reduces neutrophil adhesion activity by suppressing P-selectin and ICAM-1. In a study of PARP-deficient mice (PARP−/−), the postischemic increase in the numbers of rolling or adherent leukocytes, and platelets is significantly lower, and the serum ALT and AST activities are also lower compared to PARP+/+ mice (24). Therefore, we suggest that a similar phenomenon may occur in the present pulmonary I/R model.
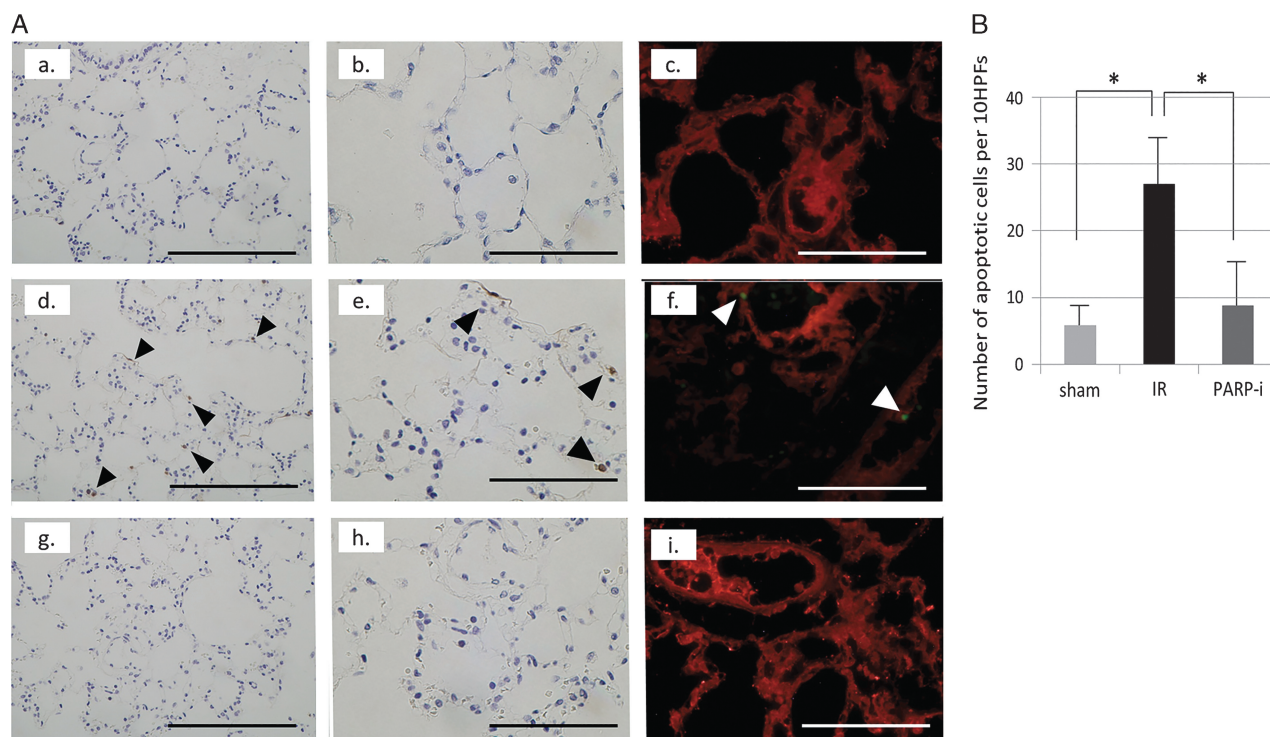
FIGURE 3. A, representative images of TUNEL staining 2 days after reperfusion (a, d, and g). The high-power field view of the same section of TUNEL staining (b, e, and h). Double fluorescent immunostaining of vascular endothelial cells (*red*) and TUNEL-positive cells (*yellow, white arrowheads*) (c, f, and i). (a, b, and c) Sham group; (d, e, and f) I/R group; (g, h, and i) PARP-i group. Some of the TUNEL-positive cells were observed in the I/R group (*arrowheads*). (a, d, g) Scale bars, 200 μm. (b, c, e, f, h, i) Scale bar, 50 μm. B, the number of TUNEL-positive cells in the lung (per 10 hpf) 2 days after reperfusion. There was a significant difference between I/R group and other 2 groups (*$P<0.05$). TUNEL, terminal deoxynucleotide transferase-mediated deoxyuridine triphosphate nick-end labeling; hpf, high-power field.

In the present study, serum TNF-α and IL-6 levels were increased after reperfusion, and PJ34 administration significantly suppressed the increase. These results are consistent with the report by Huang and colleagues (25) who showed that increased PARP activity and PARP expression in circulating mononuclear cells are positively correlated with plasma TNF-α and IL-6 levels. They also showed that PARP1 inhibition prevents the lipopolysaccharide-induced DNA binding activity of NF-κB and the decreased expression of TNF-α and IL-6. A supershift assay demonstrated that PARP is a component of the NF-κB-DNA complex. Therefore, in the present study, PJ34 may have reduced the DNA-binding activity of NF-κB and suppressed the signaling cascade of NF-κB–related cytokines, resulting in reduced serum levels of TNF-α and IL-6, which also reduce the cytokine storm and inflammatory cell infiltration in the I/R lung. The putative mechanism of PJ34 in I/R injury is shown in Figure S1 (**SDC**, http://links.lww.com/TP/B25).

Ischemia-reperfusion injury increases oxidative stress which results in DNA strand breakage, which in turn activates PARP (26). In the present study, d-ROM and BAP were used to evaluate the oxidative status. The d-ROM level is proportional to the serum hydroperoxide concentration, which reflects the peroxidation products of proteins, peptides, amino acids, lipids, and fatty acids. The d-ROM measurement is based on the ability of transition metals to catalyze, in the presence of peroxides, the formation of free radicals, which are trapped by an alchilamine. The BAP measurement is based on the ability to reduce trivalent ferric ions (27). In our study, the d-ROM level was increased 4 hr after reperfusion and remained high in the I/R group and PARP-i group. This result indicates that oxidative stress was similar in the I/R group and PARP-i group after reperfusion.

Interestingly, the BAP levels in the I/R group increased 4 hr after reperfusion but decreased by 2 days and remained low. In the PARP-i group, BAP remained at a low level 4 hr after reperfusion and increased from 2 days. Because the BAP level reflects the biologic reducing capacity, severe oxidative stress at 4 hr after reperfusion may induce serum antioxidants, resulting in the preservation of homeostasis. However, 2 days after reperfusion in the I/R group, the oxidative ability of infiltrated inflammatory cells and damaged necrotic tissue may have consumed the antioxidants, resulting in a decreased BAP level that remained low. On the other hand, in the PARP-i group, the inflammatory reaction in the tissue was low, which may have resulted in the maintenance of a high BAP level.

The detailed mechanism of BAP upregulation by PARP-is is complex and not completely understood. We believe that the present data indicate that an increased BAP level may be a favorable biomarker, indicating a sufficient amount of antioxidants in the serum during conditions of tissue damage. In addition, the oxidative stress index may be a more accurate biomarker for oxidative stress.
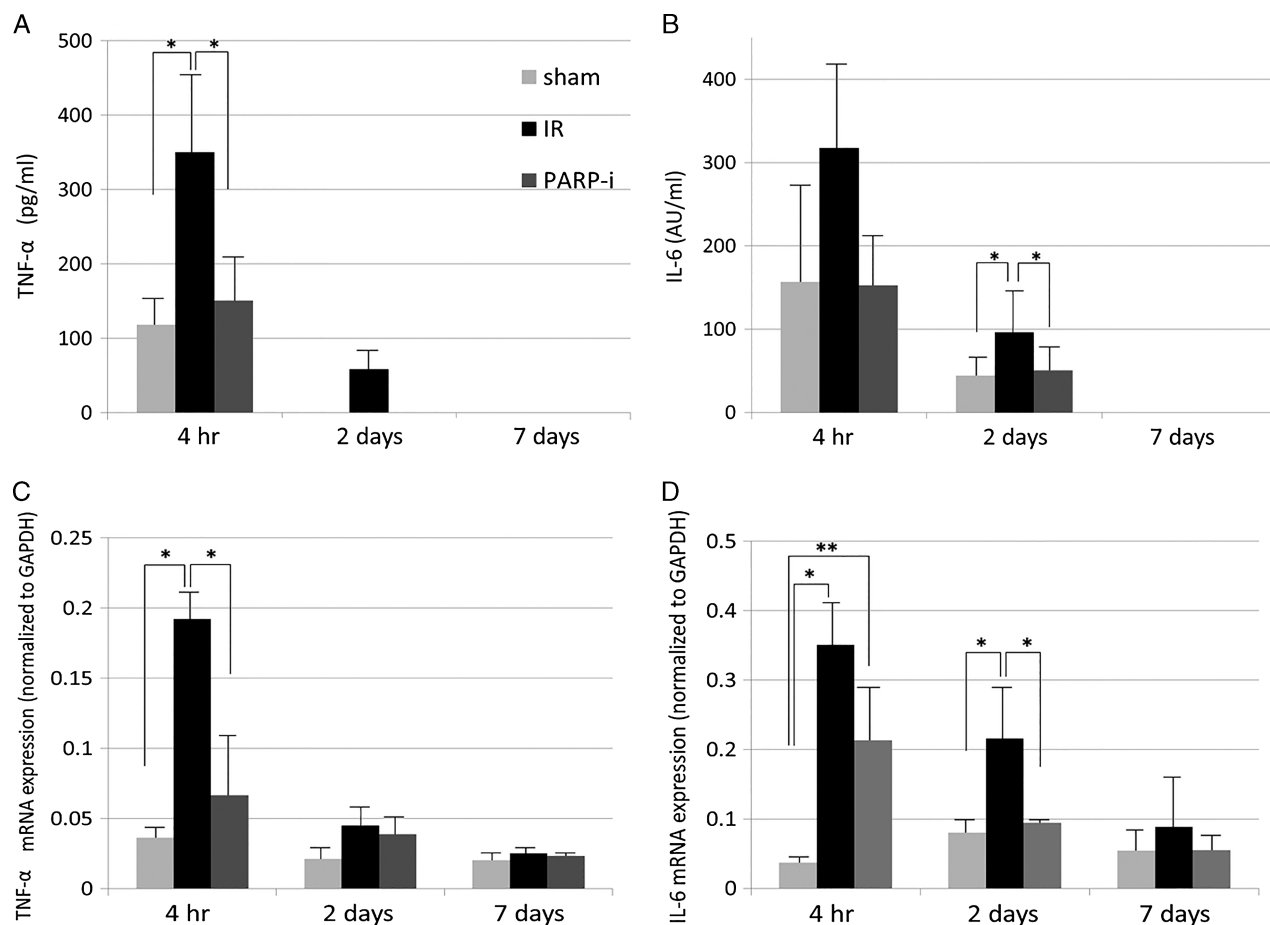
FIGURE 4.   Assessment of serum cytokine levels 4 hr, 2 days, and 7 days after reperfusion. Serum TNF-α (A) and serum IL-6 (B) 4 hr, 2 days, and 7 days after reperfusion as measured with ELISA. The mRNA expression of TNF-α (C) and IL-6 (D) in the lung 4 hr, 2 days, and 7 days after reperfusion. ELISA, enzyme-linked immunosorbent assay; TNF, tissue necrosis factor; IL, interleukin, mRNA, messenger RNA.

Our study has an important limitation. Although we aimed to confirm the tissue protective effect of the PARP-i against I/R injury in the lung, hilar clamping is different from transplantation, and our experimental setup reflects basic science. An experimental setup that involves lung preservation using PJ34-contained perfusate and an actual transplant procedure will be necessary to draw conclusions

about clinical applications of a PARP-i. On the other hand, the tissue protective effect in the warm ischemia setting indicates that a PARP-i might be useful during perfusion of harvested lungs from non–heart beating cadaveric donors.

In conclusion, the present results indicate that the PARP-i PJ34 has a tissue protective effect in the rat pulmonary I/R injury model, and the use of PJ34 may be
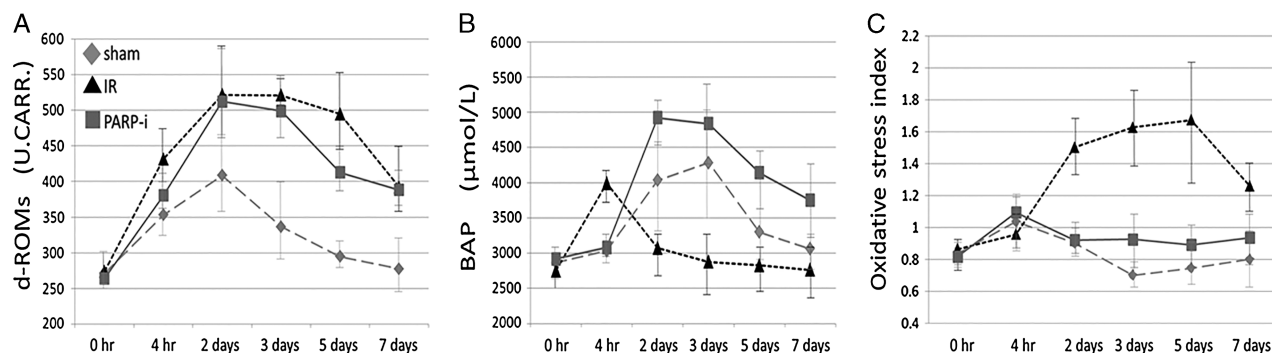
FIGURE 5.   Measurement of oxidative stress over the course of 7 days. Changes in the serum d-ROM levels (A), serum BAP levels (B), and the oxidative stress index (C) among the three groups. In the oxidative stress index, there were significant differences between I/R group and PARP-i group from 2 days after reperfusion until 7 days ($P<0.05$).(1 U. CARR.=0.08 mg H_2O_2/dL). BAP, biologic antioxidant potential. d-ROM, derivatives of reactive oxygen metabolites; U.CARR, Carratelli Units; PARP-I, PARP, poly(adenosine diphosphate-ribose) polymerase inhibitor.

correlated with the BAP. Further basic research and clinical trials will be necessary to demonstrate the usefulness of a PARP-i in lung disorders.

MATERIALS AND METHODS

Animals and Rat Pulmonary I/R Injury Model

Inbred male Wistar rats (mean, 265 g) were purchased from Kyudo Co. Ltd. (Saga, Japan) and maintained in a specific pathogen-free animal facility at Nagasaki University. All procedures were performed in accordance with the guidelines of the Institutional Animal Care and Use Committee of Nagasaki University.

The previously described rat pulmonary I/R injury model was used with modifications (28). Briefly, after inhalation of diethyl ether in a glass chamber, 0.05 mg/kg pentobarbital sodium salt was administered intraperitoneally. Anesthetized rats were orally intubated. Mechanical ventilation was set to 10 mL/kg, 90 breaths per min, and 8 mL/kg during one-lung ventilation (Harvard volume-cycled ventilator SN-480-7-10cc-2T; Shinano Seisakusyo, Tokyo, Japan). In the supine position, the left jugular vein was isolated, and a 24-G catheter was inserted. A 1-mL blood sample was collected as the pretreatment blood sample. Then, 400 U/kg heparin sodium (#3334401A6107; Mochida Pharmaceutical Co. Ltd., Tokyo, Japan) was slowly injected intravenously, followed by 0.2 mL saline (Sham group or I/R injury group) or 10 mg/kg PJ34 in a diluted solution (PARP-i group). After pretreatment, the catheter was capped and placed under the skin.

Forty minutes after the injections, a thoracotomy was performed in the left fifth intercostal space. The left lung ligament was detached to expose the left hilum. In the sham group (n=15), only a thoracotomy and left hilar isolation were performed, and the chest was closed after 1 hr. In the I/R injury group (n=15), the left main bronchus, pulmonary artery, and vein were clamped separately for 1 hr using 4-mm-long single microclamps (#1SC01; Kono Seisakusyo, Chiba, Japan). After confirming full inflation of the left lung, the chest was closed. For the I/R injury plus PARP-i group (n=15), using the previous protocol, 10 mg/kg diluted PJ34 was administered through the jugular vein 40 min before thoracotomy (19, 29). Then, the same procedures as in the I/R group were performed for the PARP-i group. The results of the dose-response study and cell viability analysis with different concentrations of PJ34 are shown in Figures S2 and S3 (**SDC**, http://links.lww.com/TP/B25).

Five rats in each group were killed at 4 hr, 2 days, and 7 days after the reperfusion to harvest organs and blood samples. In the day 7 sacrifice group, blood samples were collected from the catheter inserted in the jugular vein at 4 hr, 2 days, 3 days, 5 days, and 7 days after reperfusion. Before blood sampling, all rats were anesthetized with diethyl ether inhalation and pentobarbital sodium salt intraperitoneal injection.

Western Blotting

The protocol for sample homogenization was performed as described with partial modification (30). Denatured nuclear proteins were electrophoresed and electrotransferred to PVDF membranes. Blots were incubated with rat-specific cleaved PARP (Asp214) antibody (#9545S; Cell Signaling Technology, Tokyo, Japan) as the primary antibody at 4°C overnight. After washing, blots were incubated with horseradish peroxidase-conjugated secondary antibody for 1 hr. Blots were developed with the enhanced chemiluminescence system, and images were captured and scanned. Densitometric analysis of the bands was performed with AlphaEase Image Analysis Software (V.3.1.2).

Histologic Analysis

Resected lungs were fixed in 10% buffered formalin and embedded in paraffin. Representative sections were stained with HE and examined.

For analysis of apoptosis, paraffin sections were processed for TUNEL using an in situ apoptosis detection kit (Wako Pure Chemical Industries, Ltd., Osaka, Japan) according to the manufacturer's instructions. The number of TUNEL-positive cells was counted in ten high-power (×400) fields randomly selected from areas of severe inflammation in each rat. To assess apoptosis in detail, double fluorescent immunostaining was performed. Representative sections were treated with Proteinase K for

5 min. The sections were incubated with rat vascular endothelial cell antigen-1 (ab9774; Abcam, Tokyo, Japan) at 4°C overnight. The sections were treated with AlexaFluor647 (ab150115; Abcam) for 1 hr at 37°C. At the same time, TUNEL labeling was performed.

W/D Lung Ratio

Lung, heart, and trachea were extracted en bloc. The lung was dissected at the bilateral hilum from the heart and dissected at the level of the carina from the trachea. Lung tissue was weighed immediately as the wet lung weight, and the lung was placed in a thermostatic chamber at 60°C for 72 hr. Then, the dry lung was weighed, and the W/D ratio was calculated.

Cytokine Evaluation

Enzyme-Linked Immunosorbent Assay

Interleukin-6 was measured with a rat IL-6 enzyme-linked immunosorbent assay kit (Native form) (#27197; IBL, Gunma, Japan). According to the kit protocol, samples were measured in duplicate. Assays were performed with immobilized anti–IL-6 antibody. Plates were incubated overnight at 4°C and then washed before adding labeled antibody to each well for 60 min at room temperature. Then, each well was washed and allowed to react with 3,3′,5,5′-tetramethylbenzidine substrate for 30 min at room temperature in the dark. Absorbance was immediately measured with MULTISKAN JX (#51118230C; Thermo Scientific, Fukuoka, Japan) at a wavelength of 450 nm.

Tissue necrosis factor-α was measured with a rat TNF-α enzyme-linked immunosorbent assay kit (#27194; IBL, Gunma, Japan) according to the assay kit protocol as described above for IL-6.

RNA Extraction and TaqMan Real-Time PCR

Total RNA was extracted from the lung and kidney with TRIzol reagent (Invitrogen, Carlsbad, CA) according to the manufacturer's instructions. The RNA concentration was determined by Nanodrop ND1000 at 260 nm (Thermo Scientific). complementary DNA (cDNA) was synthesized using TaqMan reverse transcription reagents and quantified using PC707 (ASTEC Co., Ltd., Fukuoka, Japan). The primers and TaqMan probes for TNF-α, IL-6, and glyceraldehyde-3-phosphate dehydrogenase (GAPDH) mRNA were purchased from Sigma Genosys (Sigma-Aldrich, Hokkaido, Japan). The mRNA expression of TNF-α and IL-6 was determined with TaqMan real-time PCR using Lightcycler Nano (Roche Applied Science, Tokyo, Japan). Rat GAPDH was amplified as an internal control, and relative gene expression values were determined using the $2^{-\Delta\Delta CT}$ method (31). The following primer sequences were used: TNF-α: 5′-AGGAGAAGTTCCCAAATG-3′, 5′-GTATGAAGTGGCAAATCG-3′, IL-6: 5′-TTGGGACTGATGTTGTTG-3′, 5′-TGAATGACTCTGGCTTTG-3′, GAPDH: 5′-TGAGGCCGGTGCTGAGTATGT-3′, 5′-CAGTCTTCTGGGTGGCAGTGAT-3′.

Oxidative Stress Evaluation

Oxidative stress was evaluated by measuring d-ROM and BAP using Free Radical Elective Evaluator Carpe Diem (#13B2X10066W00004; Wismerll Co. Ltd., Tokyo, Japan) as described previously (32). Briefly, both tests (d-ROM and BAP) were performed in duplicate for each sample at 37°C. Serum samples were reacted with chromogenic reagent for d-ROM in the cartridge. The absorbance of the d-ROM reagent was measured at 505 nm for 5 min. To measure the BAP level, chromogenic reagent for BAP was reacted with serum sample for 5 min, and then the absorbance was measured at 505 nm. The oxidative stress index was calculated with the formula: d-ROM/BAP×8.85 (oxidative stress factor), as described previously (33).

Statistical Analysis

For comparisons among three groups, a global test of significance (Kruskal-Wallis test with Bonferroni correction to account for the number of comparisons) was performed to determine differences between median values with standard division. If a difference was significant, the Steel-Dwass test was performed. Statistical analysis was performed using SPSS statistics 21.0 (IBM, Tokyo, Japan). A P value less than 0.05 was considered indicative of a significant difference.

Additional *Materials and Methods* can be found online (**SDC**, http://links.lww.com/TP/B25).

REFERENCES

1. Ma A, Qi S. Antioxidant therapy for prevention of inflammation, ischemic reperfusion injuries and allograft rejection. *Cardiovasc Hematol Agents Med Chem* 2008; 6: 20.
2. Sodhi RK, Singh N, Jaggi AS. Poly(ADP-ribose) polymerase-1 (PARP-1) and its therapeutic implications. *Vascul Pharmacol* 2010; 53: 77.
3. Jaeschke H. Molecular mechanisms of hepatic ischemia-reperfusion injury and preconditioning. *Am J Physiol Gastrointest Liver Physiol* 2003; 284: G15.
4. Chen CF, Wang D, Hwang CP, et al. The protective effect of niacinamide on ischemia-reperfusion-induced liver injury. *J Biomed Sci* 2001; 8: 446.
5. Liaudet L, Pacher P, Mabley JG, et al. Activation of poly(ADP-ribose) polymerase-1 is a central mechanism of lipopolysaccharide-induced acute lung inflammation. *A J Respir Crit Care Med* 2002; 165: 372.
6. Mortusewicz O, Ame JC, Schreiber V, et al. Feedback-regulated poly(ADP-ribosly)ation by PARP-1 is required for rapid response to DNA damage in living cells. *Nucleic Acids Res* 2007; 35: 7665.
7. Éthier C, Tardif M, Arul L, et al. PARP-1 modulation of mTOR signaling in response to a DNA alkylating agent. *PLoS ONE* 2012; 7: e47978.
8. Cuzzocrea S, Costantino G, Zingarelli B, et al. Protective effect of poly(ADP-ribose)synthase inhibitors in zymosan-activated plasma induced paw edema. *Life Sci* 1999; 65: 957.
9. Pulido EJ, Shames BD, Selzman CH, et al. Inhibition of PARS attenuates endotoxin-induced dysfunction of pulmonary vasorelaxation. *Am J Physiol* 1999; 227(4Pt1): L769.
10. Beneke S. Poly(ADP-ribose) polymerase activity in different pathologies—the link to inflammation and infarction. *Exp Gerontol* 2008; 43: 605.
11. Xu H, Luo P, Zhao Y, et al. Iduna protects HT22 cells from hydrogen peroxide-induced oxidative stress through interfering poly(ADP-ribose) polymerase-1-induced cell death (parthanatos). *Cell Signal* 2012; 25: 1018.
12. Kaufmann SH, Desnoyers S, Ottaviano Y, et al. Specific proteolytic cleavage of poly(ADP-ribose)polymerase: an early marker of chemotherapy-induced apoptosis. *Cancer Res* 1993; 53: 3976.
13. Piper HM, Meuter K, Schafer C. Cellular mechanism of ischemia-reperfusion injury. *Ann Thorac Surg* 2003; 75: S644.
14. Ba X, Garg NJ. Signaling mechanism of poly(ADP-ribose) polymerase-1(PARP-1) in inflammatory diseases. *Am J Pathol* 2011; 178: 946.
15. Schreiber V, Dantzer F, Ame JC, et al. Poly(ADP-ribose): novel functions for an old molecule. *Nat Rev Mol Cell Biol* 2006; 7: 517.
16. Pacher P, Szabo C. Role of the peroxinitrite-poly(ADP-ribose) polymerase pathway in human disease. *Am J Pathol* 2008; 173: 2.
17. Mathews MT, Berk BC. PARP-1 inhibition prevents oxidative and nitrosative stress-induced endothelial cell death via transactivation of the VEGF receptor 2. *Arterioscler Thromb Vasc Biol* 2008; 28: 711.
18. Crawford RS, Albadawi H, Atkins MD, et al. Postischemic poly (ADP-ribose) polymerase (PARP) inhibition reduces ischemia reperfusion injury in a hind-limb ischemia model. *Surgery* 2010; 148: 110.
19. Conrad MF, Albadawi H, Stone DH, et al. Local administration of the poly ADP-ribose polymerase (PARP) inhibitor, PJ34 during hind limb ischemia modulates skeletal muscle reperfusion injury. *J Surg Res* 2006; 135: 233.
20. Couturier JY, Ding-Zhou L, Croci N, et al. 3-Aminobenzamide reduces brain infarction and neutrophil infiltration after transient focal cerebral ischemia in mice. *Exp Neurol* 2003; 184: 973.
21. Haddad M, Beray-Berthat V, Coqueran B, et al. Reduction of hemorrhagic transformation by PJ34, a poly(ADP-ribose)polymerase inhibitor, after permanent focal cerebral ischemia in mice. *Eur J Pharmacol* 2008; 588: 52.
22. Soriano FG, Pacher P, Mabley J, et al. Rapid reversal of the diabetic endothelial dysfunction by pharmacological inhibition of poly(ADP-ribose) polymerase. *Circ Res* 2001; 89: 684.
23. Shi X, Nuttall AL. Expression of adhesion molecular proteins in the cochlear lateral wall of normal and PARP-1 mutant mice. *Hear Res* 2007; 224: 1.
24. Khandoga A, Enders G, Biberthaler P, et al. Poly(ADP-ribose) polymerase triggers the microvascular mechanisms of hepatic ischemia-reperfusion injury. *Am J Physiol Gastrointest Liver Physiol* 2002; 283: G553.
25. Huang D, Yang CZ, Huang K, et al. Activation and overexpression of PARP-1 in circulating mononuclear cells promote TNF-alpha and IL-6 expression in patients with unstable angina. *Arch Med Res* 2008; 39: 775.
26. Virág L. Structure and function of poly(ADP-ribose) polymerase-1: role in oxidative stress-related pathologies. *Curr Vasc Pharmacol* 2005; 3: 209.
27. Alberti A, Bolognini L, Macciantelli D, et al. The radical cation of *N,N*-diethyl-*para*-phenylendiamine: a possible indicator of oxidative stress in biological samples. *Res Chem Intermediates* 2000; 26: 253.
28. Stone DH, Conrad MF, Albadawi H, et al. Effect of PJ34 on spinal cord tissue viability and gene expression in a murine model of thoracic aortic reperfusion injury. *Vasc Endovascular Surg* 2009; 43: 444.
29. Lenzér G, Kis B, Snipes JA, et al. Contribution of poly(ADP-ribose) polymerase to postischemic blood-brain barrier damage in rats. *J Cereb Blood Flow Metab* 2007; 27: 1318.
30. Kumar D, Schatz F, Moore RM, et al. The effect of thrombin and cytokines upon the biomechanics and remodeling of isolated amnion membrane, in vitro. *Placenta* 2011; 32: 206.
31. Rodrigues Hell RCS, Costa MM, Goes AM, et al. Local injection of BDNF producing mesenchymal stem cells increases neuronal survival and synaptic stability following ventral root avulsion. *Neurobiol Dis* 2008; 33: 290.
32. Kanaoka Y, Inagaki E, Hamanaka S, et al. Analysis of reactive oxygen metabolites (ROMs) after cardiovascular surgery as a marker of oxidative stress. *Acta Med Okayama* 2010; 64: 323.
33. Nojima J, Motoki Y, Tsuneoka H, et al. 'Oxidation stress index' as a possible clinical marker for the evaluation of non-Hodgkin lymphoma. *Br J Haematol* 2011; 155: 528.